


 Cite this: *RSC Adv.*, 2026, 16, 9108

# Boosting the extraction of humic acid from HCl-activated weathered coal catalyzed by oxygen vacancy-rich CuO nanoparticles

 Xianglei Cao,<sup>1</sup> Yongsheng Gao,<sup>2\*</sup> Zhanwen Cao,<sup>3</sup> Jia Guo,<sup>4</sup> Liugen Zhang,<sup>4</sup> Zhaojun Yang,<sup>4</sup> Kaigang Li<sup>4</sup> and Chao Yang<sup>4</sup>

The efficient extraction of humic acid (HA) from weathered coal is crucial for its high-value utilization. However, conventional methods often suffer from low extraction yields and insufficient product purity. To address these limitations, this study proposes a novel synergistic strategy combining "hydrochloric acid activation pretreatment" with "catalytic oxidation". Specifically, weathered coal was first pretreated with hydrochloric acid to enhance its hydrophilicity and remove impurities. Subsequently, the activated coal was subjected to targeted oxidative degradation using hydrogen peroxide (H<sub>2</sub>O<sub>2</sub>) catalyzed by CuO nanoparticles rich in oxygen vacancies. This synergistic process significantly enhanced the HA extraction yield from a baseline of approximately 50% in the raw coal to over 91.5% (based on the residue). Characterization results revealed that the hydrochloric acid treatment effectively improved the pore structure and surface properties of the weathered coal. Meanwhile, the oxygen vacancies in the CuO nanoparticles greatly promoted the activation of H<sub>2</sub>O<sub>2</sub> to generate hydroxyl radicals (<sup>•</sup>OH), which efficiently cleaved the macromolecular cross-linked structures in the coal. This work develops an efficient and green method for extracting HA from weathered coal and provides a new catalytic chemical pathway for the high-value utilization of coal resources.

 Received 24th December 2025  
 Accepted 10th February 2026

DOI: 10.1039/d5ra09959e

[rsc.li/rsc-advances](https://rsc.li/rsc-advances)

## 1 Introduction

Weathered coal, as an important mineral resource, is rich in humic acid (HA) with high added value, although it does not have the property of high calorific value fuel.<sup>1–4</sup> It shows broad application prospects in agriculture, environmental remediation, materials science and other fields. Efficient extraction and activation of HA is the key to realize its resource utilization.<sup>2–8</sup> However, humic substances in weathered coal usually exist in the form of large molecular weight, complex structure and low activity, resulting in low direct extraction rate and poor bioavailability. Therefore, the core way to improve the yield and quality of HA is to increase oxygen-containing functional groups and degrade macromolecular structure through activation treatment.<sup>9–13</sup>

However, single H<sub>2</sub>O<sub>2</sub> oxidation still has the problems of limited free radical generation efficiency and insufficient penetration of coal matrix hydrophobicity, which may lead to

inadequate oxidation or low selectivity of target products.<sup>14–16</sup> The introduction of catalysts is an effective strategy to solve the above bottlenecks. For example, transition metal oxides (such as CuO, TiO<sub>2</sub>, *etc.*) have been shown to significantly improve the activation efficiency of H<sub>2</sub>O<sub>2</sub>, thereby improving the extraction rate of HA.<sup>17,18</sup> Nevertheless, the existing catalytic systems still face two challenges: one is the balance between catalytic efficiency and cost-effectiveness, the exposure of active sites of traditional catalysts is limited, and the regulation of active structures such as oxygen vacancies is insufficient; the other is the neglect of raw material pretreatment. The inherent ash and impurities in weathered coal not only affect the purity of HA, but also hinder the effective mass transfer of catalytic oxidation reaction on its hydrophobic surface.<sup>14,15</sup>

In view of the above dual challenges, an innovative strategy of synergistic effect of physicochemical pretreatment and nanocatalytic oxidation was proposed in this study, aiming to simultaneously overcome the efficiency and purity bottlenecks in the extraction process of HA. Firstly, hydrochloric acid is adopted to carry out activation pretreatment on weathered coal. The step not only can effectively dissolve out ash and soluble impurities such as calcium, magnesium and the like and obviously improve the purity of the final HA product; more importantly, acid treatment can etch the surface of coal particles, increase their porosity and hydrophilicity, thus greatly improving the interfacial contact efficiency between reactants

<sup>1</sup>Xinjiang Hami Santanghu Energy Development and Construction Co., Ltd, Hami 839000, China. E-mail: 418389912@qq.com

<sup>2</sup>Xinjiang Energy (Group) Co., Ltd, Urumqi 830000, China

<sup>3</sup>Key Laboratory of Oil and Gas, School of Chemical Engineering, Xinjiang University, Urumqi 830017, China. E-mail: jerryyang1924@xju.edu.cn

<sup>4</sup>College of Chemistry and Chemical Engineering, Central South University, Changsha 410083, China


and catalysts in the subsequent reaction system.<sup>19</sup> Secondly, in the core step of catalytic oxidation, we synthesized a series of CuO nanoparticles with controllable size and morphology and rich in oxygen vacancies as catalysts. By precisely adjusting the particle size of nano-CuO and optimizing its catalytic synergistic effect with H<sub>2</sub>O<sub>2</sub>, the macromolecular network in weathered coal was selectively degraded into highly active small molecular HA. The abundant oxygen vacancy defect structure is expected to further enhance the electron transfer ability and free radical generation efficiency of the catalyst.

In this paper, the realization process and mechanism of HA enhanced extraction will be systematically described. Firstly, the regulation of hydrochloric acid pretreatment on the physical structure, chemical composition and surface properties of weathered coal was revealed; secondly, the structure–activity relationship between the oxygen vacancy concentration of CuO nanoparticles with different sizes and their catalytic performance was clarified, and the catalytic mechanism of CuO nanoparticles in the oxidation of weathered coal by H<sub>2</sub>O<sub>2</sub> was explored. This study provides a new idea of pretreatment purification-catalytic oxidation integration for the efficient and high-quality extraction of HA from weathered coal.

## 2 Experimental section

### 2.1 Experimental materials

Weathered coal in Xinjiang was used as the research object. After the coal sample is taken back, it is crushed, screened to below 60 mesh, and dried at 120 °C for 3 h to obtain the coal sample for the experiment, which is placed in a drying vessel for storage.

### 2.2 Experimental reagents

Copper acetate (Cu(CH<sub>3</sub>COO)<sub>2</sub>·H<sub>2</sub>O), potassium hydroxide (KOH), concentrated hydrochloric acid (HCl, 37%), hydrogen peroxide (H<sub>2</sub>O<sub>2</sub>, 30%), absolute ethanol (C<sub>2</sub>H<sub>5</sub>OH) and other reagents were analytically pure and were not further purified. The water used in the experiment was distilled water.

### 2.3 Synthesis of CuO with different particle size

Weigh 5 mmol cupric acetate into 100 mL ethanol/water mixed solution, and stir vigorously for 30 min. After complete dissolution, 25 mL of ethanol/water mixed solution dissolved in 20 mmol NaOH was poured into the above solution and refluxed for 1 h in a water bath at 90 °C. After the temperature is naturally reduced, the mixture is centrifugally collected and washed three times with water and ethanol respectively. The obtain black powder is that CuO particle. The ratios of ethanol/water were 0 : 100, 50 : 50, 75 : 25 and 100 : 0, respectively. According to the ratios of ethanol, the CuO series were named CuO-0, CuO-50, CuO-75 and CuO-100, respectively.

### 2.4 Weathered coal pretreatment (activation and desalination)

Weigh 50 g of weathered coal powder into a beaker, and add 100 mL of mixed solution of distilled water and hydrochloric

acid. The suspension was stirred with a glass rod and activated in a 95 °C water bath for 30 min. After natural cooling and sedimentation, the supernatant was removed and the same amount of distilled water was added, twice a day for five days. And drying at 120 °C to obtain a weathered coal sample activated by hydrochloric acid.

### 2.5 Extraction method of HA

Weigh 2 g of weathered coal and 0.45 g of KOH, and disperse them in a 100 mL beaker containing 30 mL of distilled water. Stir the mixture continuously for 30 minutes. After sufficient dispersion, 80 mg of catalyst was added thereto and stirred for 30 min. Then 1 mL of 30% H<sub>2</sub>O<sub>2</sub> solution was added dropwise to the above dispersion (2 drops per second) and stirring was continued for 1 h. Centrifuge the supernatant, wash the residue once, and combine the washings with the supernatant. The pH of the supernatant was adjusted to about 1 with dilute hydrochloric acid solution, and HA was separated by centrifugation. The HA and residue were dried and weighed to record the weight.

All the above experimental operations were completed in a constant temperature laboratory at 25 °C.

## 3 Results and discussion

HA was extracted from weathered coal by alkali dissolution and acid precipitation method, and the effects of catalyst and oxidant were investigated. As can be seen from Fig. 1, the extraction amount of HA was 1.013 g and the extraction rate was about 50% without the addition of oxidant and catalyst. The extraction amount of HA was only slightly increased after adding oxidant, which proved that single hydrogen peroxide did not play an oxidation role in the oxidation process, which may be related to the obstruction of free radical transfer process. However, the amount of HA increased to 1.329 g after the addition of CuO catalyst, which was about 30% higher than that of the experimental group without catalyst. The results showed

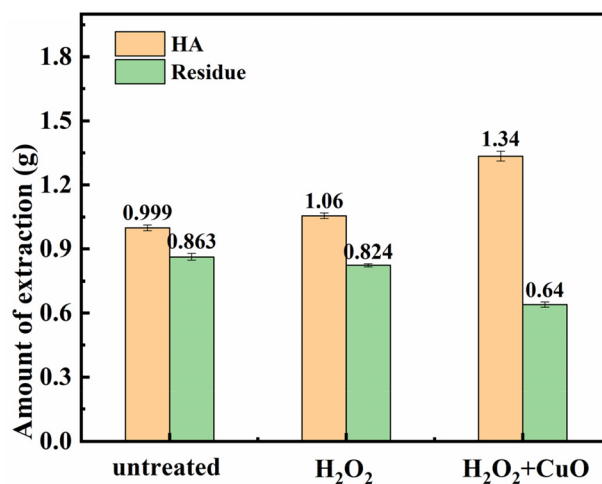


Fig. 1 Effect of H<sub>2</sub>O<sub>2</sub> and CuO on HA extraction by alkali extraction and acid precipitation (condition: 25 °C, KOH: 450 mg, coal: 2 g).



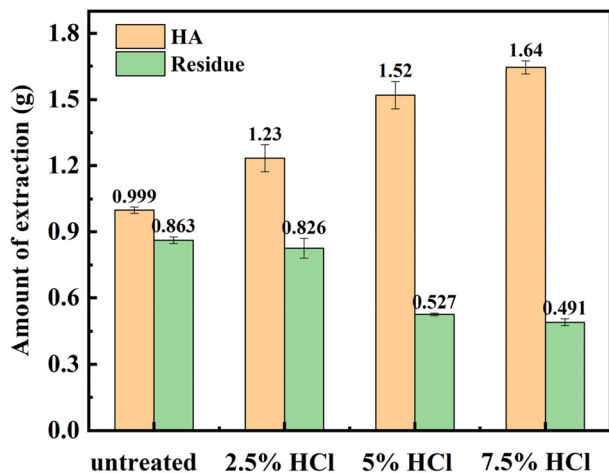


Fig. 2 HA extraction amount of coal samples activated by different concentrations of hydrochloric acid (condition: 25 °C, KOH: 450 mg, coal: 2 g, H<sub>2</sub>O<sub>2</sub>: 1 mL).

that the single H<sub>2</sub>O<sub>2</sub> had no oxidation effect under the experimental conditions, but the catalytic oxidation effect was obvious in the presence of CuO, and the extraction rate of HA increased from 50% to 65%.

Dilute hydrochloric acid treatment can improve the acidic groups on the surface of weathered coal, increase the hydrophilicity of HA molecules, and accelerate the dissolution of HA molecules. The HA extraction amount of the hydrochloric acid activated coal sample is shown in Fig. 2.

As shown in Fig. 2, after the weathered coal sample is activated by hydrochloric acid, the extraction amount of HA is gradually increased under the conditions of alkali dissolution

and acid precipitation without adding oxidant and catalyst. When the concentration of hydrochloric acid is 7.5%, the extraction amount of HA is 1.613 g, which is 60% higher than that of the original weathered coal. The results show that the activation of hydrochloric acid can effectively promote the dissolution and precipitation of HA.

In order to explore the changes of weathered coal samples in the process of hydrochloric acid activation, the coal samples before and after hydrochloric acid activation were characterized by SEM, EDS and contact angle.

SEM reflects the micro-morphology information of coal samples. Fig. 3a and b are SEM images of the original weathered coal sample. The coal sample has large particles and smooth surface. Fig. 3c and d are SEM images of the weathered coal activated by 5% hydrochloric acid. The coal sample particles are seriously agglomerated, which is caused by rewetting and drying. Moreover, after the activation of hydrochloric acid, the particle size of the coal sample is slightly reduced, and there are micropores on the surface of the particle. In contrast, hydrochloric acid activation can reduce the particle size of weathered coal to a certain extent, and can corrode some micropores on the surface of coal particles (Fig. 4).

EDS is used to analyze the type and content of elements in the micro-area of the material. As shown in the figure, the contents of Na, Mg, Al, S, Ca, Mn and other elements in the weathered coal decreased significantly after being activated by 5% hydrochloric acid. The results show that 5% hydrochloric acid activation and longtime soaking dissolution have obvious effects on reducing the salinity of weathered coal.

Contact angle test can characterize the hydrophilicity of weathered coal samples. The smaller the angle between the water droplets on the surface of the sample and the plane of the coal sample, the better the hydrophilicity and wettability. The

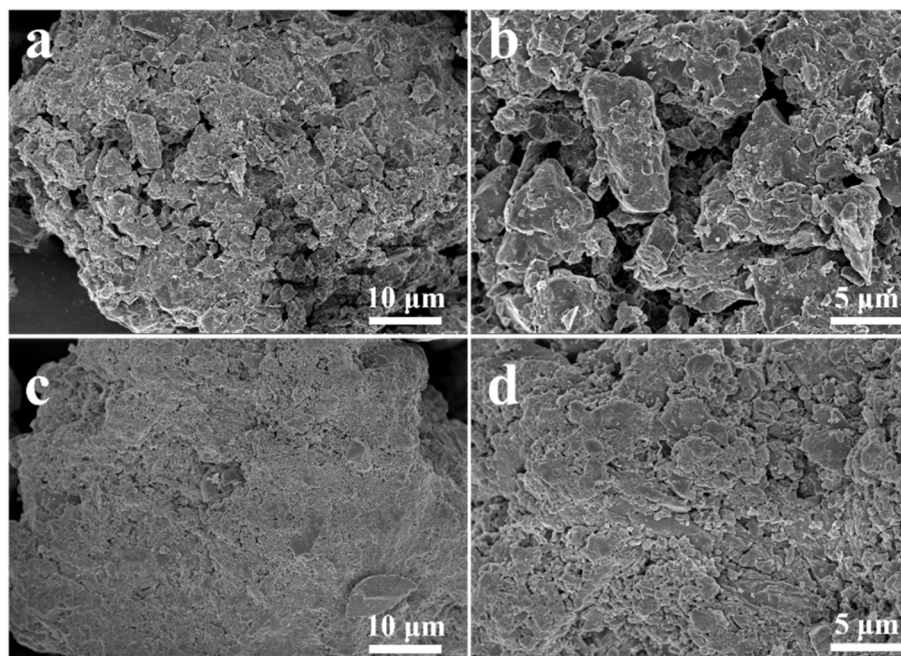


Fig. 3 SEM of (a) and (b) original weathered coal; (c) and (d) weathered coal activated by 5% hydrochloric acid.



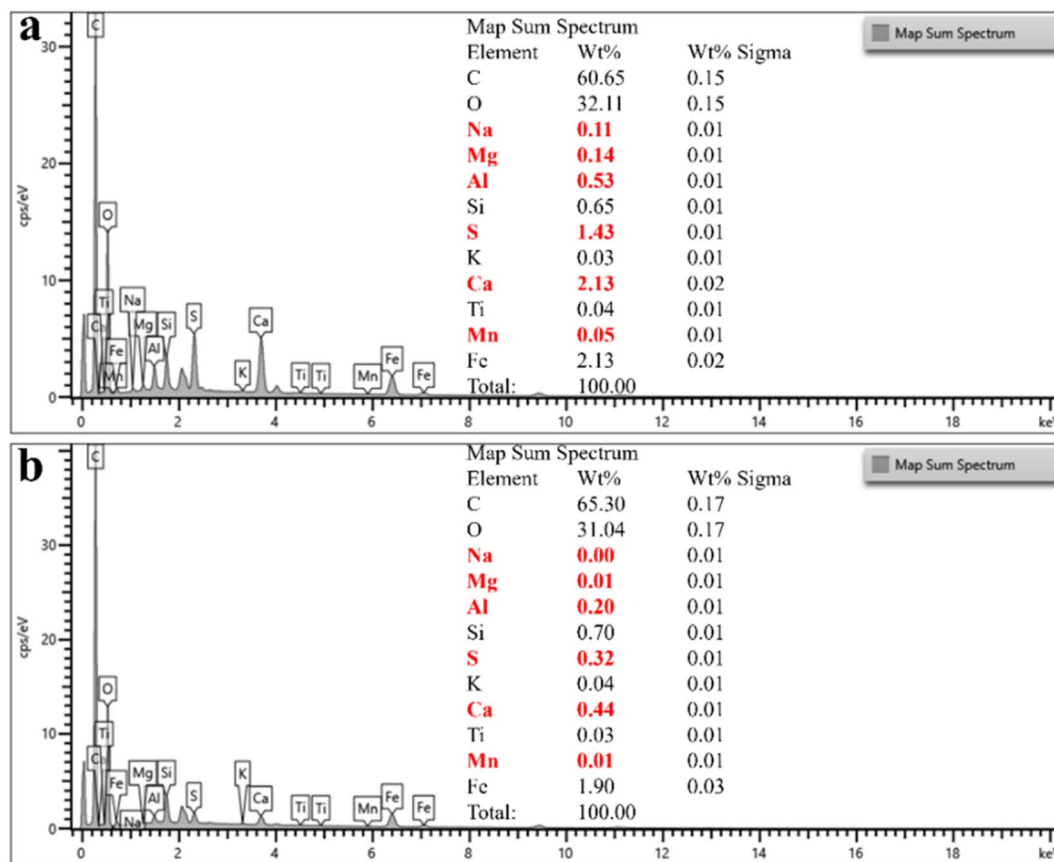


Fig. 4 EDS element distribution: (a) original weathered coal; (b) weathered coal activated by 5% hydrochloric acid.

contact angle test of the original sample of weathered coal and the sample activated by hydrochloric acid is shown in Fig. 5. The contact angle of the original sample of weathered coal is 122.6°, which means that the original weathered coal is hydrophobic, has poor wettability, and has large dispersion and dissolution resistance in water, which hinders mass transfer. While the

contact angle of the weathered coal activated by 5% hydrochloric acid is 21.3°, and the weathered coal has good wetting effect and hydrophilicity. The results of contact angle test show that hydrochloric acid activation can modify the surface of weathered coal, make it hydrophilic,<sup>19</sup> and promote the transfer of HA molecules from solid phase to liquid phase in alkali dissolution (Table 1).

In order to clarify the change of main elements before and after hydrochloric acid activation, the elemental analysis of weathered coal and hydrochloric acid activated coal was carried out. The H content increased from 2.674% to 2.896%, which was due to the increase of proton content on the surface of coal samples during hydrochloric acid activation. Proton as

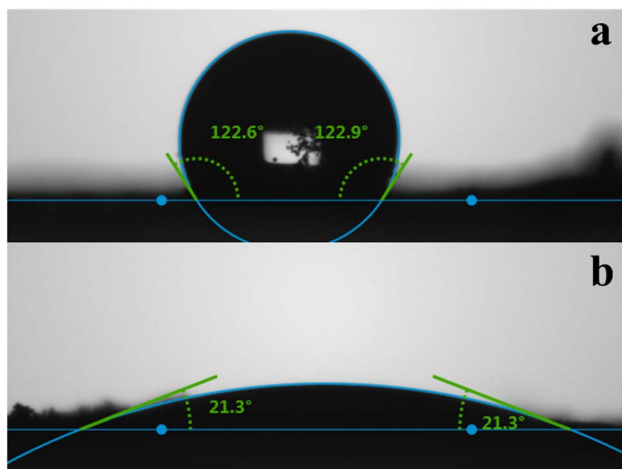


Fig. 5 Contact angle test: (a) original weathered coal; (b) weathered coal activated by 5% hydrochloric acid.

Table 1 Element analysis of original weathered coal sample and weathered coal activated by 5% hydrochloric acid

Elements	Content (original weathered coal sample)	Content (weathered coal activated by 5% hydrochloric acid)
C	39.08%	45.57%
H	2.674%	2.896%
O	37.23%	38.595%
N	1.5%	1.6%
S	2.751%	1.190%



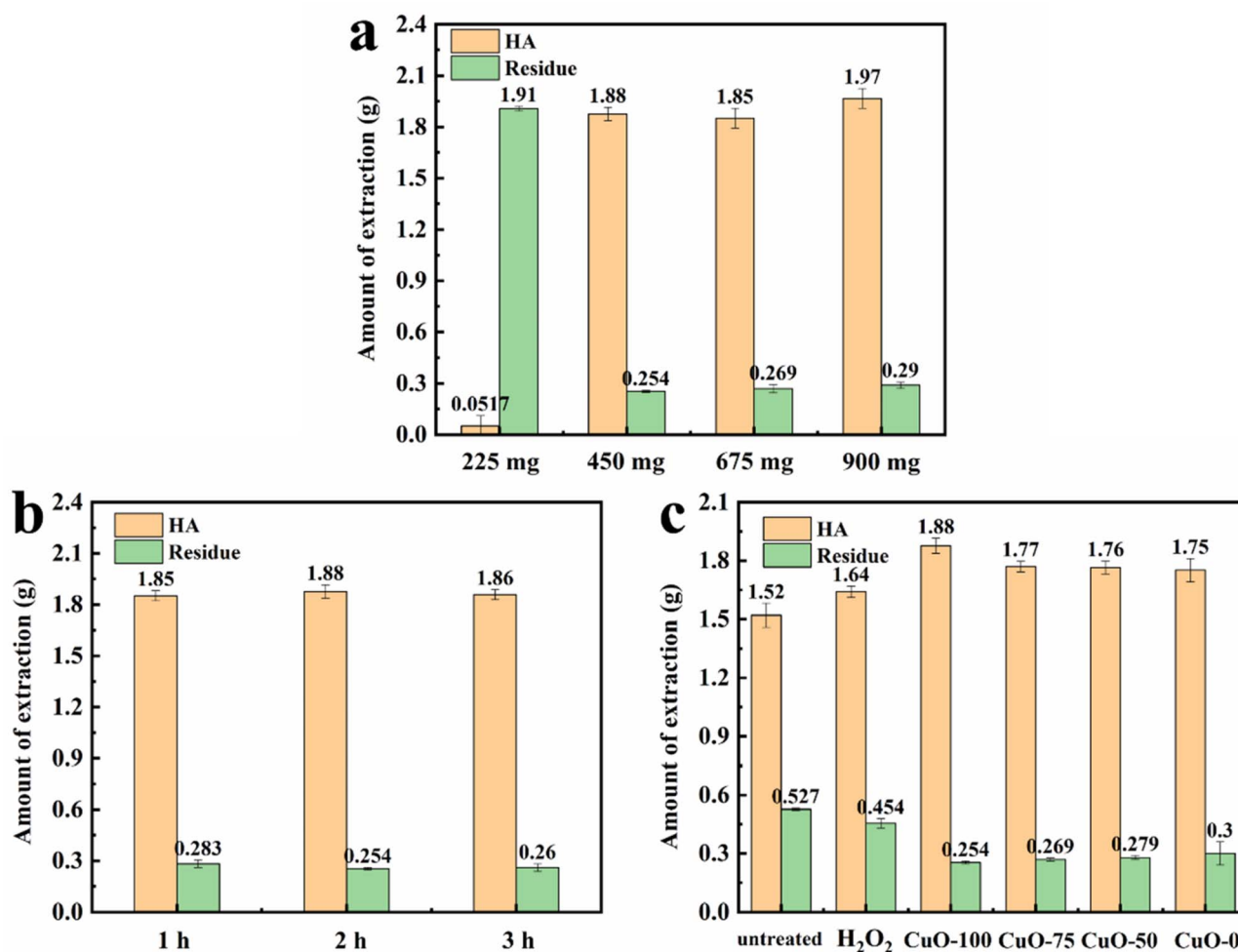


Fig. 6 (a) HA yield at different alkali concentrations; (b) HA yield at different catalytic oxidation time; (c) HA yield catalyzed by CuO with different particle sizes (condition: 25 °C, coal: 2 g, H<sub>2</sub>O<sub>2</sub>: 1 mL).

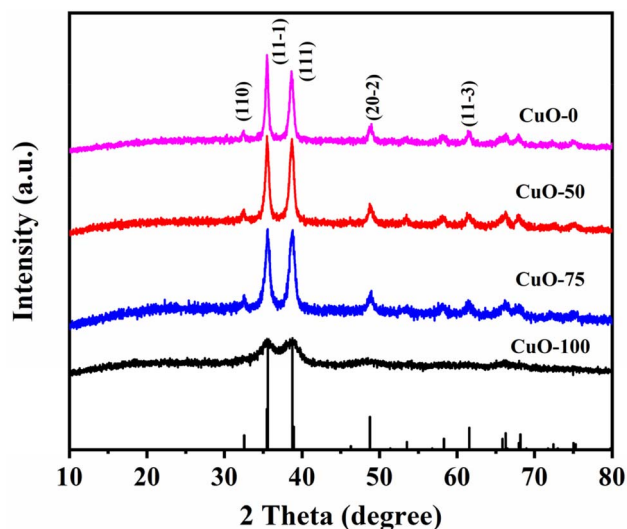


Fig. 7 XRD pattern of CuO series catalyst.

a hydrophilic group can increase the wettability and hydrophilicity of coal samples. Not only that, but other elements not tested in the table were also reduced by 6.7% after hydrochloric acid activation.

The above characterization shows that after the weathered coal sample is treated with 5% hydrochloric acid solution, the metal ions in the coal sample are dissolved and removed in the treatment process, which can reduce the content of metal salts in the weathered coal and improve the purity of HA. Moreover, hydrochloric acid activation can reduce the particle size of coal particles, increase the surface micropores of particles, increase the number of surface protons, and ultimately improve the hydrophilic wettability of coal samples, promote the dissolution of HA molecules in alkali liquor, and increase the yield of HA from 50% to 75.5% (based on the residue).

The extraction process of HA was optimized by using the coal sample activated by 5% hydrochloric acid as raw material. Fig. 6a is a histogram of the amount of HA extracted by the alkali-extraction and acid-precipitation method under different alkali concentrations. HA was hardly dissolved when the amount of alkali was 225 mg/30 mL. However, when the amount



of alkali was increased to 450 mg, the yield of HA was increased to 1.889 g, and with the further increase of the amount of alkali, the yield of HA was limited. The addition amount of 450 mg of alkali is optimal in view of economy. Fig. 6b is a histogram of HA production for different catalytic oxidation times. The catalytic oxidation rate involved in this process is rapid, with HA being substantially oxidized within 1 hour and peaking at 2 hours. As the time continues to extend to 3 hours, the foam on the surface of the dispersion has begun to carbonize, which may be the main reason for the low extraction of HA. Therefore, 2 hours is the best time for catalytic oxidation, and 1 hour is also acceptable if the economic and time costs are considered. Four kinds of CuO catalysts with different particle sizes were

prepared and applied to the extraction of HA by alkali-extraction and acid-precipitation method. As shown in Fig. 6c, the CuO catalyst prepared in anhydrous ethanol has the best catalytic effect, with HA extraction of 1.889 g, which is about 5% higher than other CuO catalysts.

In order to explore the structure of the catalyst and its role in the catalytic process, a series of CuO were characterized by XRD and SEM.

The type of substance and crystal structure can be judged by XRD, and the XRD spectrum of CuO series catalyst is shown in Fig. 7. The diffraction patterns of the series of CuO in the figure are consistent with the standard card PDF#48-1548.<sup>20</sup> According to the ethanol content in the solvent during the synthesis of

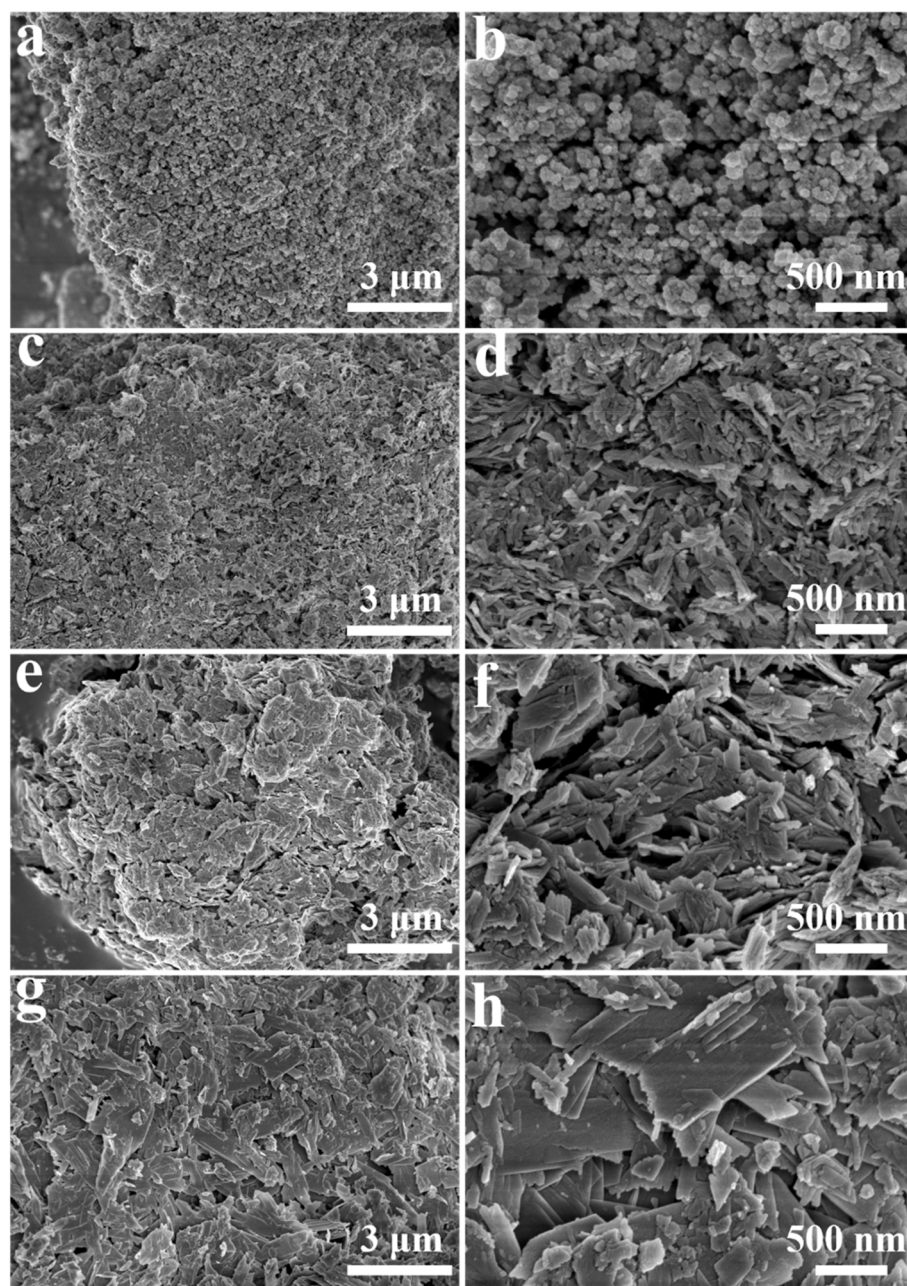


Fig. 8 SEM images of CuO series catalysts: (a) and (b) CuO-100; (c) and (d) CuO-75; (e) and (f) CuO-50; (g) and (h) CuO-0.



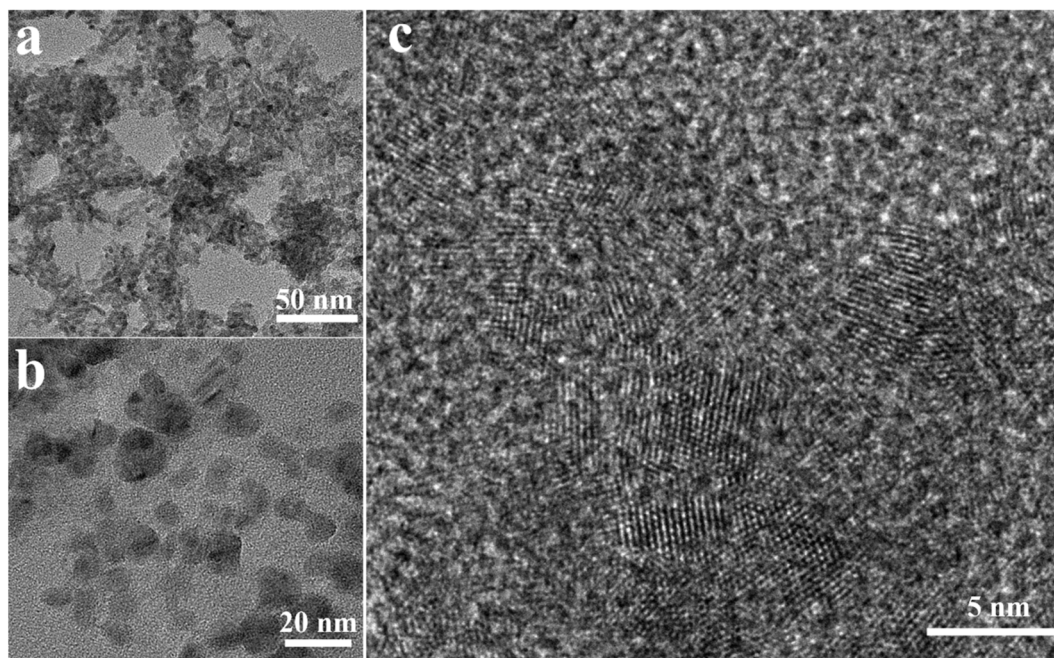


Fig. 9 TEM image of CuO-100.

CuO from top to bottom, the crystallinity decreases with the increase of ethanol content. When the synthesis solvent is absolute ethanol, the crystallinity of CuO decreased. The crystallinity of the CuO catalyst series, as determined by XRD, decreases in the following order: 99.57%, 99.89%, 99.69%, and 91.12%.<sup>21</sup> In addition, the dielectric constant of the solvent also has a greater impact on the size of the material synthesis. The dielectric constant of ethanol is lower than that of water, so the number of particles obtained is more and the final size is smaller.

In order to further verify the size rule of CuO, the SEM of CuO series catalysts was characterized, as shown in Fig. 8. CuO-100

exhibits a granular morphology with particle diameters ranging from 100 to 200 nm. CuO-75 displays a rod-like shape, with lengths between 3 and 4  $\mu\text{m}$ . As the ethanol content in the synthesis solvent further decreases, CuO-50 and CuO-0 evolve into a sheet-like structure, which increases in size with lower ethanol content. These distinct morphologies observed by SEM are, in essence, the macroscopic outcomes of how crystallites aggregate and grow under different solvent conditions. This structural evolution is corroborated by XRD analysis, which reveals a corresponding trend at the crystallographic level: the calculated crystallite sizes for the CuO series decrease in the order of 22.2 nm, 16.9 nm, 13.6 nm, and 5.4 nm.<sup>22</sup>

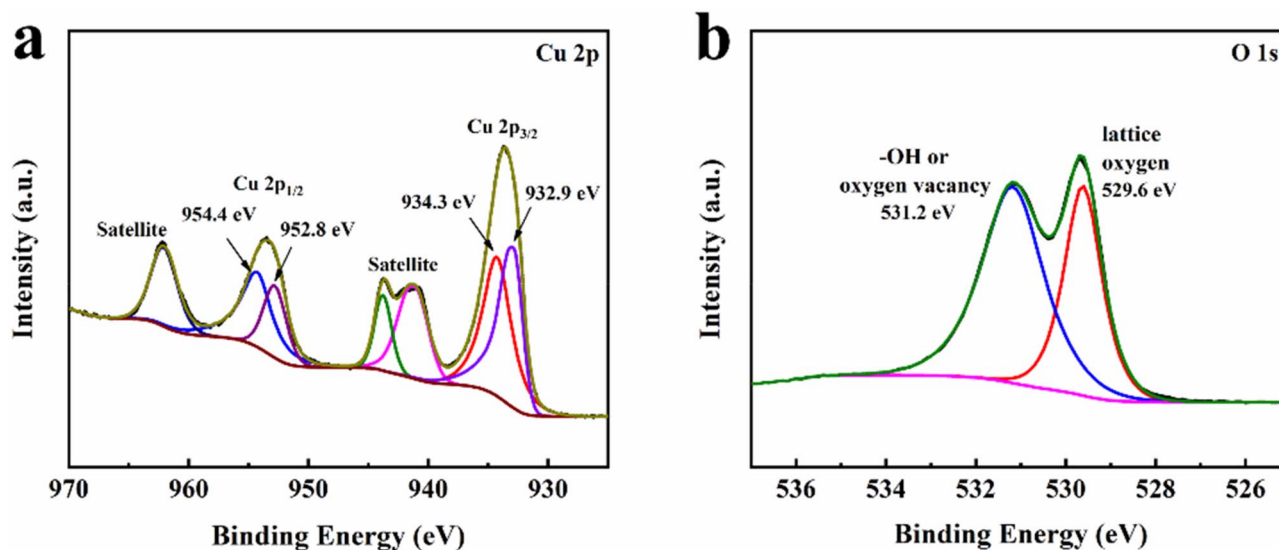


Fig. 10 (a) Cu 2p and (b) O 1s fine spectra of CuO-100.



CuO-100 has the best performance in the catalytic oxidation of HA, and its structural characteristics are worth further exploring. Therefore, the CuO-100 catalyst was characterized by TEM, XPS, O<sub>2</sub>-TPD and EPR to reveal its structure–activity relationship.

CuO particles larger than 100 nm appear in the SEM images, which may be caused by the agglomeration of CuO particles. After complete dispersion, nanoparticles around 10 nm in diameter are revealed in the TEM image (Fig. 9a). Fig. 9b is a large magnification TEM image, and the outline of CuO can be clearly seen. Fig. 9c shows the lattice fringes of CuO-100, and the measured span of the lattice fringes is mostly about 0.253 nm, which is consistent with the (11-1) crystal plane of CuO.<sup>23</sup> The lattice fringes are ordered locally, but limited by the size of CuO particles, they are disordered on a larger scale (tens of nanometers), which is consistent with the poor crystallinity or even amorphous state shown in the XRD pattern of CuO-100.

XPS can be used to characterize the composition and valence of elements on the surface of catalysts, which is of great

significance for the analysis of catalyst structure. Fig. 10a shows the Cu 2p orbital fine spectrum of CuO-100, in which the characteristic peaks at 932.9 and 934.3 eV are assigned to the Cu 2p<sub>3/2</sub> orbital, while the characteristic peaks at 952.8 and 954.4 eV are assigned to the Cu 2p<sub>1/2</sub> orbital. The two peaks represent the presence of Cu<sup>2+</sup>.<sup>24</sup> The characteristic peak at 529.6 eV in the O 1s spectrum corresponds to the lattice oxygen and is dominated by the Cu–O bond. The characteristic peak at 531.2 eV is mainly corresponding to the hydroxyl groups in the bound water and the oxygen vacancies in CuO. These results suggest that CuO-100 may contain oxygen vacancies, which play a positive role in the adsorption and activation of oxygen-containing radicals.

It is generally recognized that the key to the oxidation process is that the catalyst stimulates the oxidant to generate highly active free radicals, often termed as the free radical reaction pathway. The role of free radical pathway in the oxidation of humic substances was investigated by quenching ·OH with TBA and quenching ·O<sup>2-</sup> with P-BQ, as showed in

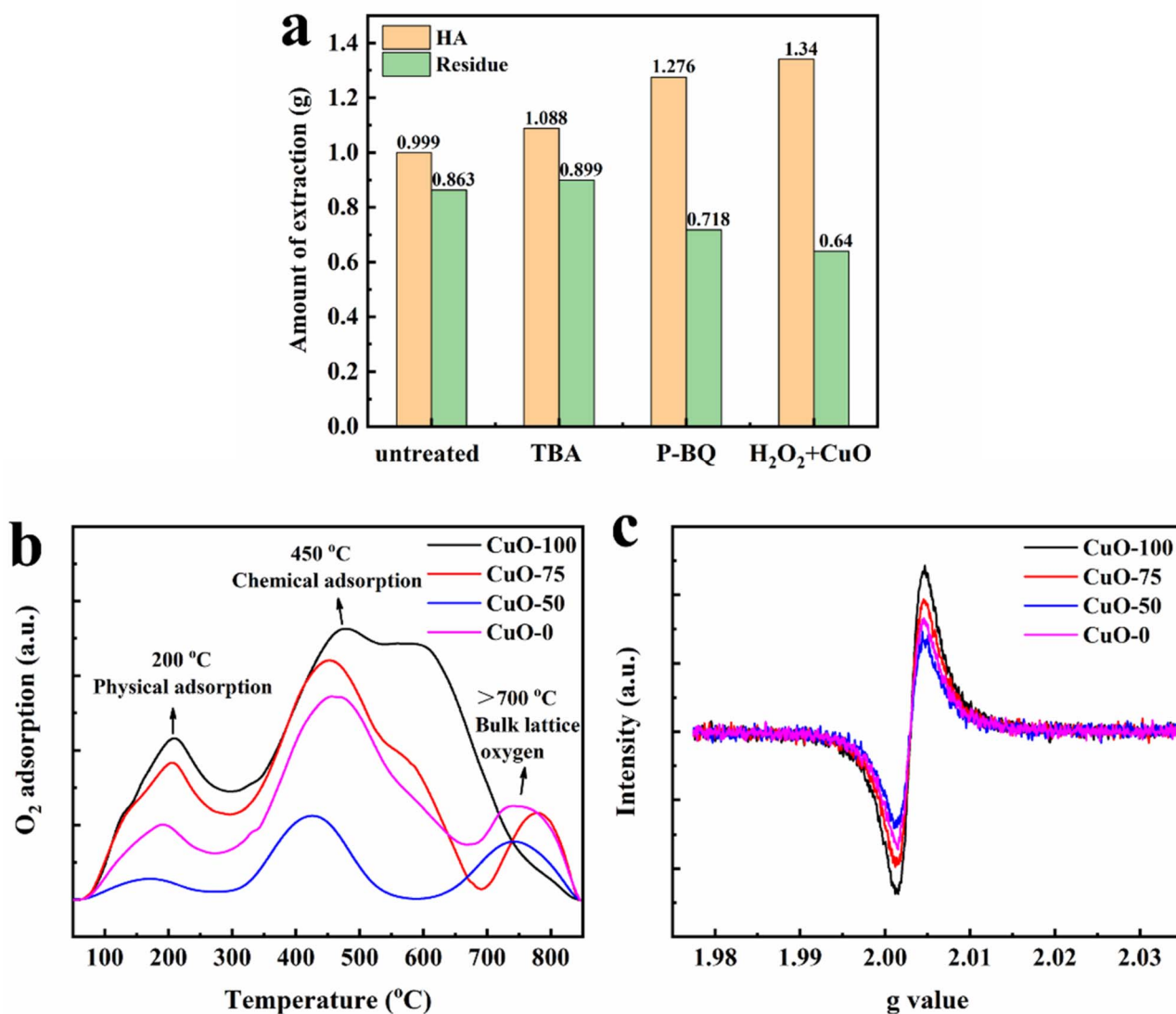


Fig. 11 (a) Effects of the quenching agents on HA extraction; (b) O<sub>2</sub>-TPD curve of CuO-100 and (c) EPR curve of CuO-100.



Fig. 11a. The effects of  $\cdot\text{OH}$ ,  $\cdot\text{O}^{2-}$ , and other pathways were assessed to be 74.1%, 18.8%, and 7.1%. The results show that  $\cdot\text{OH}$  is the predominant reactive oxygen species in this system.<sup>25,26</sup>

In order to further verify the oxygen adsorption sites and oxygen vacancies on the surface of CuO-100, its  $\text{O}_2$ -TPD and EPR were tested. Fig. 11b is an  $\text{O}_2$  temperature-programmed desorption curve of a series of CuO catalysts, which characterizes the  $\text{O}_2$  adsorption sites on the surface of CuO. As shown, three distinct desorption peaks were observed at 200, 450, and 750 °C. Among them, the low temperature adsorption peak at 200 °C represents physical adsorption, the electronic structure of  $\text{O}_2$  has not changed, and the reaction activity is low. The middle temperature adsorption peak at 400 °C represents the chemical adsorption, which diffuses to the active site through physical adsorption to form a chemical connection, and the large desorption peak proves that the  $\text{O}_2$  on the active site has good mobility. The high temperature region above 700 °C represents the bulk lattice oxygen, and the desorption peak in this region represents the destruction of the catalyst structure. Compared with other catalysts, CuO-100 has stronger physical adsorption and chemical adsorption, and also shows good stability in the high temperature region, which is consistent with its catalytic performance.

Electron paramagnetic resonance (EPR) measurements were performed on the CuO sample, and the results are shown in Fig. 11c. A typical single Lorentzian line is observed at  $g = 2.003$  in the spectrum, which is attributed to the characteristic peak of oxygen vacancies (OVs).<sup>27</sup> The intensity of the peak is proportional to the concentration of oxygen vacancies on the surface of the catalyst. CuO-100 has abundant oxygen vacancies, which can adsorb and transfer more oxygen radicals. The presence of oxygen vacancies can promote the adsorption and decomposition of  $\text{H}_2\text{O}_2$  to OH on the surface of CuO catalyst, thus effectively improving the surface oxygen mobility and catalytic activity.<sup>28–30</sup>

## 4 Conclusion

In this paper, the pretreatment of weathered coal activated by hydrochloric acid and CuO catalytic oxidation were used to enhance the extraction of HA from weathered coal.

1. Under the optimal conditions with 450 mg of alkali, the CuO-100 catalyst, and a reaction time of 2 h, the extraction rate of HA was increased from 50% to 91.5% (based on the residue).

2. Hydrochloric acid activation can increase the proton concentration on the surface of weathered coal particles, thus improving its hydrophilicity and promoting the dissolution of HA molecules, and reduce the salinity of weathered coal in the stage of hydrochloric acid soaking. Quenching experiments show that the dominant free radical is  $\cdot\text{OH}$ , and the abundant oxygen adsorption sites and oxygen vacancies on the CuO surface promote the activation of  $\text{H}_2\text{O}_2$  to form  $\cdot\text{OH}$ .

3. The purity of the humic acid product is improved through dilute hydrochloric acid activation and soaking, and a coupling strategy of pretreatment and catalytic oxidation is provided for enhancing the extraction of the humic acid.

## Conflicts of interest

The authors declare that they have no known competing financial interests or personal relationships that could have appeared to influence the work reported in this paper.

## Data availability

The data that support the findings of this study are available from the corresponding author upon reasonable request.

## Acknowledgements

We acknowledged the financial support from Xinjiang Hami Santanghu Energy Development and Construction Co., Ltd, Xinjiang Energy (Group) Co., Ltd and the third batch of key talent introduction plan in Xinjiang Uygur Autonomous Region.

## References

- 1 X. Li, Research on sustainable development and utilization of coal resources in Xinjiang, *Henan Sci. Technol.*, 2009, 11–12.
- 2 J. Krumins, Z. Yang, Q. Zhang, M. Yan and M. Klavins, A study of weathered coal spectroscopic properties, *Energy Procedia*, 2017, 128, 51–58.
- 3 J. Kus, M. Misz-Kennan and ICCP, Coal weathering and laboratory (artificial) coal oxidation, *Int. J. Coal Geol.*, 2017, 171, 12–36.
- 4 W. Xia, J. Yang and C. Liang, Investigation of changes in surface properties of bituminous coal during natural weathering processes by XPS and SEM, *Appl. Surf. Sci.*, 2014, 293, 293–298.
- 5 K. Ampong, M. S. Thilakarathna and L. Y. Gorim, Understanding the Role of Humic Acids on Crop Performance and Soil Health, *Front. Agron.*, 2022, 4, 848621.
- 6 O. Bezuglova and A. Klimenko, Application of Humic Substances in Agricultural Industry, *Agronomy*, 2022, 12, 584.
- 7 S. Delfino, R. Tognetti, E. Desiderio and A. Alvino, Effect of foliar application of N and humic acids on growth and yield of durum wheat, *Agron. Sustainable Dev.*, 2005, 25, 183–191.
- 8 G. Ferrara and G. Brunetti, Influence of foliar applications of humic acids on yield and fruit quality of table grape cv. Italia, *OENO One*, 2008, 42, 79–87.
- 9 X. Chen, L. Zhang, G. Wang, X. Zhao, S. Sun, Y. Ren, Y. Tian, Y. Guo, R. Zhang, Q. Wang, B. Davronbek and X. Su, Catalytic pyrolysis of waste biomass via coal fly ash for synergistic production of cost-effective artificial humic acid, *Bioresour. Technol.*, 2026, 442, 133682.
- 10 G. Cheng, Z. Niu, C. Zhang, X. Zhang and X. Li, Extraction of Humic Acid from Lignite by KOH-Hydrothermal Method, *Appl. Sci.*, 2019, 9, 1356.
- 11 A. Veeken, K. Nierop, V. d. Wilde and B. Hamelers, Characterisation of NaOH-extracted humic acids during composting of a biowaste, *Bioresour. Technol.*, 2000, 72, 33–41.



- 12 Q. Sun, C. Xu, Z. Geng and D. She, Extraction and characterization of humic acid with high bio-activity by mechanical catalytic treatment, *Ind. Crops Prod.*, 2023, **206**, 117623.
- 13 F. Yang, S. Zhang, K. Cheng and M. Antonietti, A hydrothermal process to turn waste biomass into artificial fulvic and humic acids for soil remediation, *Sci. Total Environ.*, 2019, **686**, 1140–1151.
- 14 K. C. Christoforidis, M. Louloudi and Y. Deligiannakis, Effect of humic acid on chemical oxidation of organic pollutants by iron(II) and H<sub>2</sub>O<sub>2</sub>: A dual mechanism, *J. Environ. Chem. Eng.*, 2015, **3**, 2991–2996.
- 15 Z. Yang, L. Gong and P. Ran, Preparation of nitric humic acid by catalytic oxidation from Guizhou coal with catalysts, *Int. J. Min. Sci. Technol.*, 2012, **22**, 75–78.
- 16 N. Fatima, A. Jamal, Z. Huang, R. Liaquat, B. Ahmad, R. Haider, M. I. Ali, T. Shoukat, Z. A. Alothman, M. Ouladsmame, T. Ali, S. Ali, N. Akhtar and M. Sillanpää, Extraction and Chemical Characterization of Humic Acid from Nitric Acid Treated Lignite and Bituminous Coal Samples, *Sustainability*, 2021, **13**, 8969.
- 17 L. Zhou, L. Yuan, B. Zhao, Y. Li and Z. Lin, Structural characteristics of humic acids derived from Chinese weathered coal under different oxidizing conditions, *PLoS One*, 2019, **14**, e0217469.
- 18 Y. Guo, C. Ma, P. Hui, J. Yang and L. Wang, Extraction and characterization of humic acid from weathered coal, *Chin. J. Environ. Eng.*, 2017, **11**, 3153–3160.
- 19 C. Wang, S. Leng, H. Guo, L. Cao and J. Huang, Acid and alkali treatments for regulation of hydrophilicity/hydrophobicity of natural zeolite, *Appl. Surf. Sci.*, 2019, **478**, 319–326.
- 20 S. J. Singh, Y. Y. Lim, J. J. L. Hmar and P. Chinnamuthu, Temperature dependency on Ce-doped CuO nanoparticles: a comparative study via XRD line broadening analysis, *Appl. Phys. A*, 2022, **128**, 188.
- 21 S. W. Oh, H. J. Bang, Y. C. Bae and Y.-K. Sun, Effect of calcination temperature on morphology, crystallinity and electrochemical properties of nano-crystalline metal oxides (Co<sub>3</sub>O<sub>4</sub>, CuO, and NiO) prepared via ultrasonic spray pyrolysis, *J. Power Sources*, 2007, **173**, 502–509.
- 22 V. Uvarov and I. Popov, Metrological characterization of X-ray diffraction methods at different acquisition geometries for determination of crystallite size in nano-scale materials, *Mater. Charact.*, 2013, **85**, 111–123.
- 23 D. A. Svintsitskiy, T. Y. Kardash, O. A. Stonkus, E. M. Slavinskaya, A. I. Stadnichenko, S. V. Koscheev, A. P. Chupakhin and A. I. Boronin, In Situ XRD, XPS, TEM, and TPR Study of Highly Active in CO Oxidation CuO Nanopowders, *J. Phys. Chem. C*, 2013, **117**, 14588–14599.
- 24 F. Ansari, S. Sheibani and M. Fernandez-García, Surface modification of Cu<sub>2</sub>O-CuO photocatalyst on Cu wire through decorating with TiO<sub>2</sub> nanoparticles for enhanced visible light photocatalytic activity, *J. Alloys Compd.*, 2022, **919**, 165864.
- 25 K. Wang, C. Guo, J. Li, Y. Wang, Y. Xing, P. Li, Z. Wang and J. Wang, Efficient degradation of tetracycline via N-doped carbon derived from discarded PET plastics by boosting peroxymonosulfate activation and singlet oxygen generation, *Chem. Eng. J.*, 2025, **507**, 160653.
- 26 Q. Mei, J. Sun, D. Han, B. Wei, Z. An, X. Wang, J. Xie, J. Zhan and M. He, Sulfate and hydroxyl radicals-initiated degradation reaction on phenolic contaminants in the aqueous phase: Mechanisms, kinetics and toxicity assessment, *Chem. Eng. J.*, 2019, **373**, 668–676.
- 27 Z. Wang, C. Guo, K. Wang, J. Li and J. Wang, Facile preparation of Fe<sub>2</sub>O<sub>3</sub>@Co-MOF with oxygen-rich vacancies from waste PET bottles for ethylbenzene oxidation, *J. Alloys Compd.*, 2025, **1038**, 182511.
- 28 Y. Ding, J. Wang, S. Xu, K.-Y. A. Lin and S. Tong, Oxygen vacancy of CeO<sub>2</sub> improved efficiency of H<sub>2</sub>O<sub>2</sub>/O<sub>3</sub> for the degradation of acetic acid in acidic solutions, *Sep. Purif. Technol.*, 2018, **207**, 92–98.
- 29 X. Hu, J. Wang, J. Wang, Y. Deng, H. Zhang, T. Xu and W. Wang,  $\beta$  particles induced directional inward migration of oxygen vacancies: Surface oxygen vacancies and interface oxygen vacancies synergistically activate PMS, *Appl. Catal., B*, 2022, **318**, 121879.
- 30 Z. Tan, J. Zhang, Y.-C. Chen, J.-P. Chou and Y.-K. Peng, Unravelling the Role of Structural Geometry and Chemical State of Well-Defined Oxygen Vacancies on Pristine CeO<sub>2</sub> for H<sub>2</sub>O<sub>2</sub> Activation, *J. Phys. Chem. Lett.*, 2020, **11**, 5390–5396.

